This appendix is available online at https://github.com/alherm/asymmetric_block_offers.

APPENDIX A
MATHEMATICAL REPRESENTATION OF ASYMMETRIC BLOCK OFFERS

This appendix provides the mathematical expression of the asymmetric block offers beginning with down-regulation, which is similar to equations (1) but with $A_{dc} = 0$:

$$\Big\{ r^{\text{dn}}_{dct} \leq P^{\text{rsp}}_{dc} o_{dct}, \quad \forall d, c, t \tag{11a}$$

$$r^{\text{up}}_{dct} \leq P^{\text{rb}}_{dc} o_{dct}, \quad \forall d, c, t \tag{11b}$$

$$\sum_{\tau=t}^{t+T^{\text{rsp}}_{dc}-1} r^{\text{dn}}_{dc\tau} \geq T^{\text{rsp}}_{dc} P^{\text{rsp}}_{dc} (o_{dct} - o_{dc,t-1}), \quad \forall d, c, t \tag{11c}$$

$$\sum_{\tau=t+T^{\text{rsp}}_{dc}}^{t+T^{\text{rsp}}_{dc}+T^{\text{rb}}_{dc}-1} r^{\text{up}}_{dc\tau} \geq T^{\text{rb}}_{dc} P^{\text{rb}}_{dc} (o_{dct} - o_{dc,t-1}), \quad \forall d, c, t \leq |T| - T^{\text{rsp}}_{dc} \tag{11d}$$

$$\sum_{\tau=t}^{t+T^{\text{rsp}}_{dc}-1} r^{\text{up}}_{dc\tau} \leq T^{\text{rb}}_{dc} P^{\text{rb}}_{dc} (1 - (o_{dct} - o_{dc,t-1})), \forall d, c, t \tag{11e}$$

$$\sum_{\tau=t+T^{\text{rsp}}_{dc}}^{t+T^{\text{rsp}}_{dc}+T^{\text{rb}}_{dc}-1} r^{\text{dn}}_{dc\tau} \leq T^{\text{rsp}}_{dc} P^{\text{rsp}}_{dc} (1 - (o_{dct} - o_{dc,t-1})) \tag{11f}$$

$$, \forall d, c, t \leq |T| - T^{\text{rsp}}_{dc} \Big\} \text{ if } A_{dc} = 0.$$

APPENDIX B
SUFFICIENT CONDITIONS

The additional sufficient conditions to be included in the MI-SOCP OPF model are listed below:

$$\hat{s}_{njt} = s_{nt} + \sum_{h:h \to n} \hat{s}_{hnt}, \quad \forall n > j \in \Phi_n, t \tag{12a}$$

$$\hat{v}_{nt} - \hat{v}_{jt} = 2\text{Re}(\overline{Z}_{nj} \hat{s}_{njt}), \quad \forall n > j \in \Phi_n, t \tag{12b}$$

$$\text{Re}(\overline{Z}_{nj} \hat{s}_{njt}) \leq 0, \quad \forall n > j \in \Phi_n, t \tag{12c}$$

$$\hat{v}_{nt} \leq \overline{V}^{\text{sq}}_{n}, \quad \forall n, t, \tag{12d}$$

where $\hat{s}_{njt} = \hat{p}_{njt} + j\hat{q}_{njt}$ is a linear approximation of the complex line flows $s_{njt} = p_{njt} + jq_{njt}$, and $\overline{Z}_{nj} = R_{nj} - jX_{nj}$ is the complex conjugate line impedance. $s_{nt} = p_{nt} + jq_{nt}$ is the complex nodal apparent power injection. Besides, $\hat{v}_{nt}$ is a linear approximation of the squared nodal voltage. The notation $\sum_{h:h \to n}$ means the sum of all lines originating in node n. These sufficient conditions are quite mild, as long as there is no combined active and reactive reverse power flow on any line. The reverse power flow can be either active or reactive but not both[11].

[11]We found out that due to numerical issues with the used solver, convergence is achieved much faster if the right-hand side of equation (12c) is replaced with a small positive number. This will not affect the tightness of the achieved solution in any significant way.

APPENDIX C
DATA FOR ILLUSTRATIVE EXAMPLE

This appendix presents the input data for the illustrative example (6-bus network). In Fig. 7 the single line diagram of the 6-bus network is given. The feeder has two conventional generators and 3 DR units. The line connecting nodes 3 and 4 has a limited capacity, and might be congested.

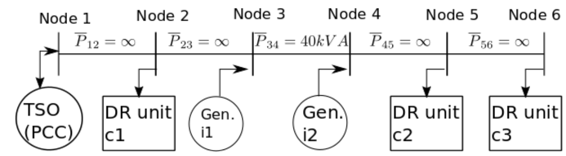

Fig. 7. Illustrative example: 6-bus radial feeder, including two local conventional generators i_1 and i_2, and three DR units c_1 to c_3. The capacity of all lines is unlimited, except the line connecting buses 3 and 4 whose capacity is 40 kVA.

In Fig. 8, the day-ahead market outcomes are given for the local conventional generators on the 6-bus feeder, as well as for the loads of the DR units. The day-ahead market outcomes have a peak in power consumption between hours 12 and 26. The line between nodes 3 and 4 is congested during peak hours. The asymmetric block offers provided by the three DR units are given in Table II, where each DR unit offers 4 different blocks to the DSO. The offer prices for these blocks are constant through time and given together with the other applicable prices in Table III.

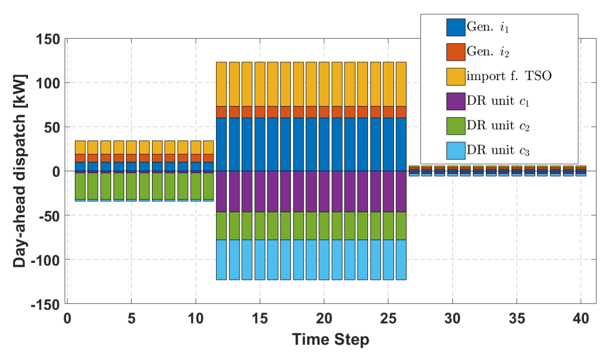

Fig. 8. Illustrative example: The input data, consisting of the day-ahead market outcomes in terms of active power. This market does not consider reactive power trading.

TABLE II
ILLUSTRATIVE EXAMPLE: THE ASYMMETRIC BLOCK OFFERS PROVIDED BY DR UNITS

DR unit	Offer	P^{rsp}_{dc}	P^{rb}_{dc}	T^{rsp}_{dc}	T^{rb}_{dc}	A_{dc}
c_1	d_1	13	17	13	9	1
	d_2	17	13	9	13	0
	d_3	10	10	20	21	1
	d_4	17	10	9	20	0
c_2	d_1	17	8	9	29	0
	d_2	8	17	29	9	1
	d_3	13	15	13	11	1
	d_4	15	13	11	13	0
c_3	d_1	12	15	15	11	1
	d_2	15	12	11	15	0
	d_3	11	13	18	14	1
	d_4	13	11	14	18	0

TABLE III
THE PRICES FOR UP- AND DOWN-REGULATION OFFERS PROVIDED BY TSO AND LOCAL DERS FOR BOTH THE ILLUSTRATIVE EXAMPLE AND THE CASE STUDY.

Resource*	Up offer price [¢/(kW-30min)]	Down offer price [¢/(kW-30min)]
Gen. i_1 and i_2	35	10
TSO	21	19
DR units c_1 to c_3	25	16

*We assume the same prices for active and reactive regulation offers. These prices are constant over time.

TABLE IV
IEEE 37-BUS TEST CASE: THE ASYMMETRIC BLOCK OFFERS PROVIDED BY DR UNITS

DR unit	Offer	P_{dc}^{rsp}	P_{dc}^{rb}	T_{dc}^{rsp}	T_{dc}^{rb}	A_{dc}
c_1	d_1	85	75	12	18	1
	d_2	72	65	13	17	0
	d_3	62	53	14	16	1
	d_4	52	43	15	15	0
	d_5	44	35	16	14	1
	d_6	32	23	17	13	0
	d_7	25	16	18	12	1
	d_8	14	5.8	19	11	0
c_2	d_1	91	11.5	18	11	0
	d_2	84	24.5	17	12	1
	d_3	76	33.5	16	13	0
	d_4	66	43.5	15	14	1
	d_5	56	53.5	14	15	0
	d_6	46	63.5	13	16	1
	d_7	36	73.5	12	17	0
	d_8	20	83.5	11	18	1
c_3	d_1	83	25.5	12	17	1
	d_2	75	34.5	13	16	0
	d_3	63	43.3	14	15	1
	d_4	53	53.3	15	14	0
	d_5	43	63.3	16	13	1
	d_6	33	73.35	17	12	0
	d_7	23	83.35	18	11	1
	d_8	13	93.35	19	10	0
c_4	d_1	102	1.55	18	10	0
	d_2	92	24.5	17	11	1
	d_3	82	33.5	16	12	0
	d_4	75	43.5	15	13	1
	d_5	65	53.5	14	14	0
	d_6	52	63.5	13	15	1
	d_7	45	73.5	12	16	0
	d_8	35	83.5	11	17	1

APPENDIX D
DATA FOR CASE STUDY: THE IEEE 37-BUS SYSTEM

This appendix gives all the input data for the 37-bus case study of section IV. The offer prices from all DR units, local conventional generators and TSO are provided in Table III. All asymmetric block offers by the four DR units are listed in Table IV. For Case A, the first three offers of each unit are used, while in Case B all 8 offers for each unit are considered. Fig. 10a depicts the active power loads at each node of the system. Fig. 10b shows the reactive power loads at each node. The dispatch of the local generators and the import from the TSO at the PCC is given in Fig. 10c.

APPENDIX E
EXTRA RESULTS FOR THE IEEE 37-BUS SYSTEM

In this appendix, some extra results of the congestion management mechanism obtained from the IEEE 37-bus case

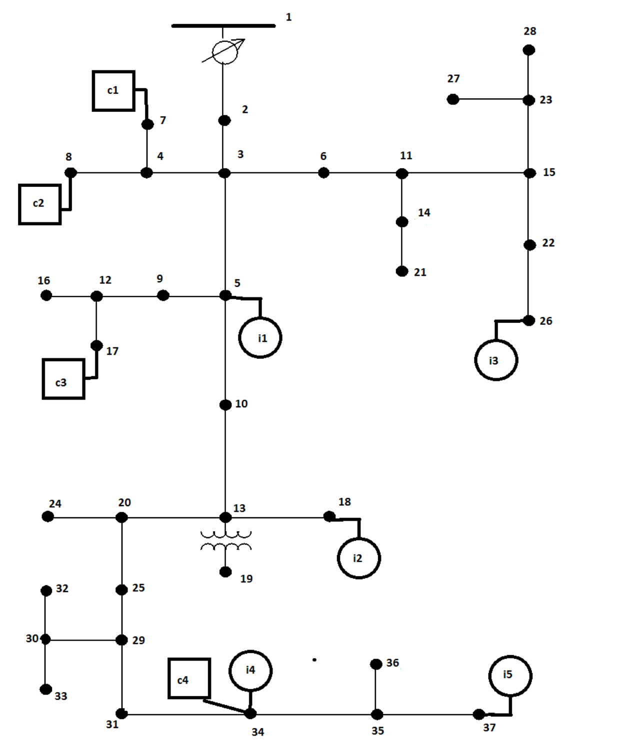

Fig. 9. The diagram for the IEEE 37-bus test feeder with local generators and DR units. Note: The bus numbers have been changed compared to the original test case in [26].

study in section IV-B are presented. These results are the re-dispatch of the local conventional generators, re-dispatch of import/export from the TSO and the dispatch of the asymmetric blocks.

The results obtained for Case A for all three OPF models are presented in Fig. 11. Likewise, the optimal results achieved in Case B for the three OPF models are presented in Fig. 12, with Fig. 12a showing the re-dispatch outcome for the linear lossless model, and Fig. 12b showig the re-dispatch for the linear model with loss approximation, and 12c showing the re-dispatch for the SOCP model. Comparing the dispatch of asymmetric blocks from the lossless MILP-OPF model and the one with loss approximation, it is observed that the same blocks are dispatched for both Cases A and B. There are minor differences in the re-dispatch of conventional generators and the import/export at the PCC due to the active power losses.

The re-dispatch results of the congestion management mechanism using the MI-SOCP OPF model are given in Fig. 11c and 12c. It is worth noticing that the asymmetric blocks dispatched in this model are quite different compared to those in MILP models.

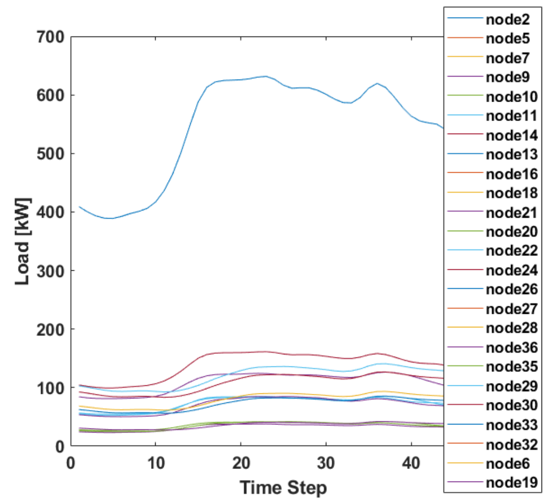

(a) Active power loads

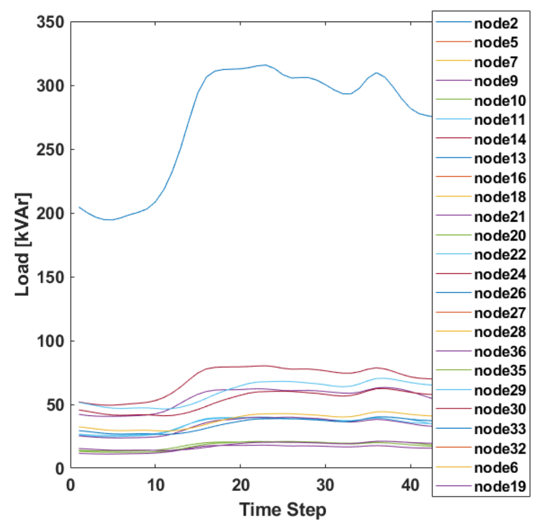

(b) Reactive power loads.

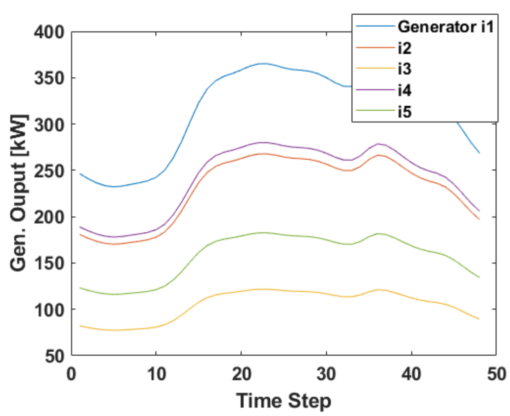

(c) Day-ahead schedule of the five conventional generators.

Fig. 10. IEEE 37-bus case study input data.

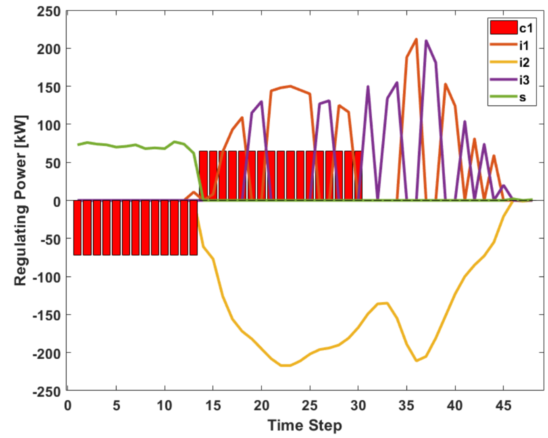

(a) MILP-OPF (lossless)

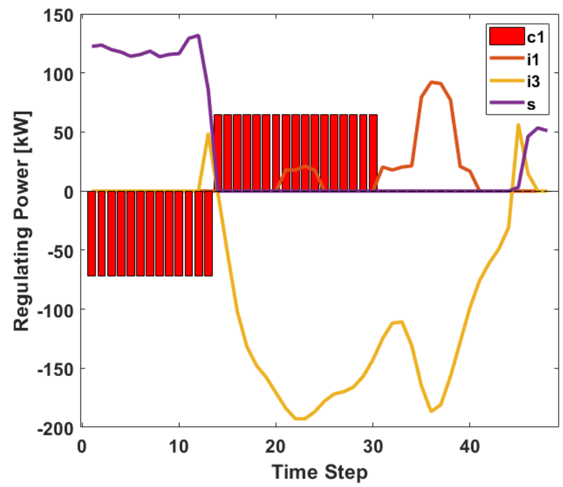

(b) MILP-OPF with loss approximation

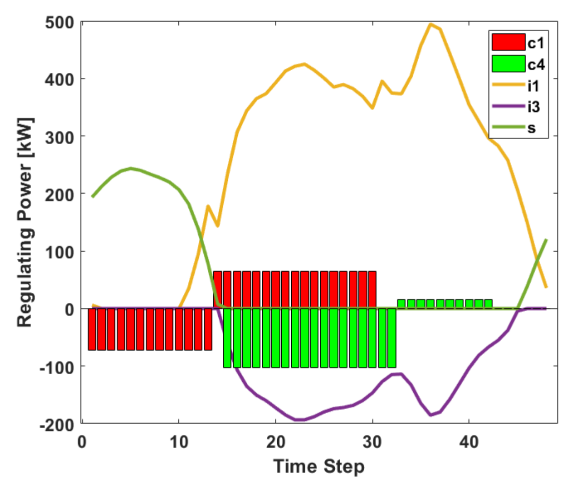

(c) MI-SOCP OPF

Fig. 11. IEEE 37-bus test case: Re-dispatch outcomes obtained from Case A with the three different OPF models.

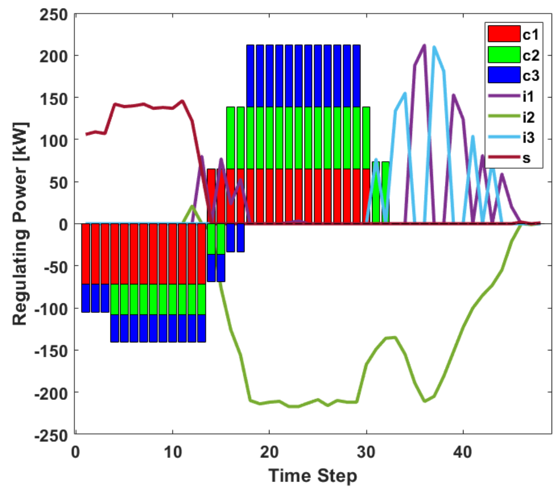

(a) MILP-OPF (lossless)

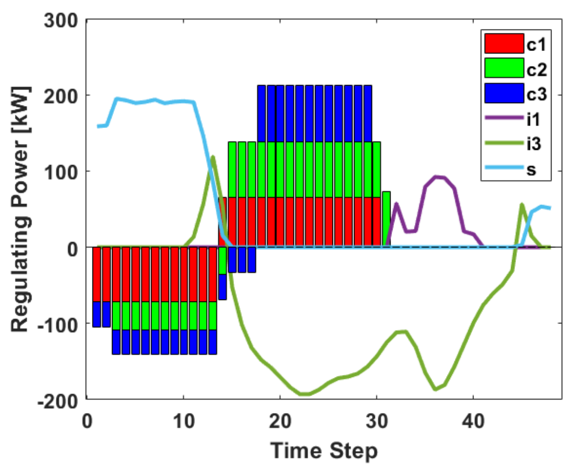

(b) MILP-OPF with loss approximation

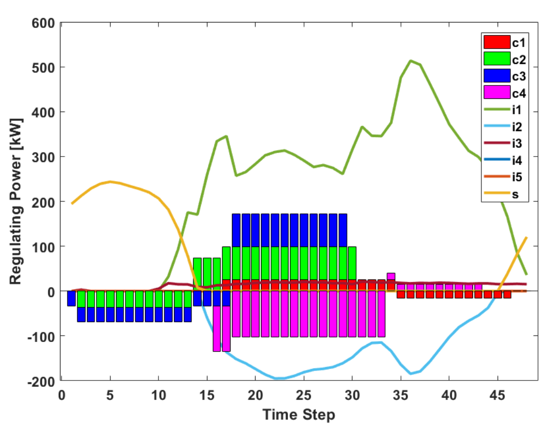

(c) MI-SOCP OPF

Fig. 12. IEEE 37-bus test case: Re-dispatch outcomes obtained from Case B with the three different OPF models.